

Domain evolution with electric field and delineation of extrinsic contributions in (K, Na, Li)(Nb, Ta, Sb)O₃ single crystal

Junjun Wang, Limei Zheng, Bin Yang, Zhenlin Luo, Xiaoyan Lu, Gang Liu, Rui Zhang, Tianquan Lv, and Wenwu Cao

Citation: *Applied Physics Letters* **107**, 072902 (2015); doi: 10.1063/1.4928756

View online: <http://dx.doi.org/10.1063/1.4928756>

View Table of Contents: <http://scitation.aip.org/content/aip/journal/apl/107/7?ver=pdfcov>

Published by the AIP Publishing

Articles you may be interested in

Phase transition sequence in Pb-free 0.96(K_{0.5}Na_{0.5})_{0.95}Li_{0.05}Nb_{0.93}Sb_{0.07}O₃-0.04BaZrO₃ ceramic with large piezoelectric response

Appl. Phys. Lett. **107**, 032902 (2015); 10.1063/1.4926874

Temperature dependence of dielectric and electromechanical properties of (K,Na)(Nb,Ta)O₃ single crystal and corresponding domain structure evolution

J. Appl. Phys. **116**, 044105 (2014); 10.1063/1.4891718

Displacement of Ta-O bonds near polymorphic phase transition in Li-, Ta-, and Sb-modified (K, Na)NbO₃ ceramics

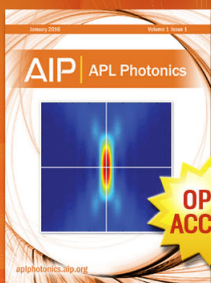
Appl. Phys. Lett. **104**, 242905 (2014); 10.1063/1.4884381

Effect of Ta content on the phase transition and piezoelectric properties of lead-free (K_{0.48}Na_{0.48}Li_{0.04})(Nb_{0.995-x}Mn_{0.005}Ta_x)O₃ thin film

J. Appl. Phys. **111**, 024110 (2012); 10.1063/1.3680882

Piezoelectric properties in perovskite 0.948 (K_{0.5} Na_{0.5}) Nb O₃ – 0.052 Li Sb O₃ lead-free ceramics

J. Appl. Phys. **100**, 104108 (2006); 10.1063/1.2382348



Launching in 2016!

The future of applied photonics research is here

OPEN ACCESS

AIP | APL Photonics

Domain evolution with electric field and delineation of extrinsic contributions in (K, Na, Li)(Nb, Ta, Sb)O₃ single crystal

Junjun Wang,¹ Limei Zheng,^{1,a)} Bin Yang,^{1,a)} Zhenlin Luo,² Xiaoyan Lu,³ Gang Liu,⁴ Rui Zhang,¹ Tianquan Lv,¹ and Wenwu Cao^{1,5}

¹Department of Physics, Condensed Matter Science and Technology Institute, Harbin Institute of Technology, Harbin 150080, China

²Department of Materials Science and Engineering, University of Science and Technology of China, Hefei 230026, China

³School of Civil Engineering, Harbin Institute of Technology, Harbin 150001, China

⁴Center for High Pressure Science and Technology Advanced Research, Shanghai 201203, China

⁵Department of Mathematics and Materials Research Institute, The Pennsylvania State University, University Park, Pennsylvania 16802, USA

(Received 19 June 2015; accepted 7 August 2015; published online 20 August 2015)

Extrinsic contributions play an important role in the functionalities of ferroelectric materials, while domain structure evolution is crucial for understanding the extrinsic dielectric and piezoelectric responses. In this work, domain configuration changes with an electric field applied along [001]_C in the tetragonal (K, Na, Li)(Nb, Sb, Ta)O₃ single crystal were studied by means of polarizing light microscopy. Results show that parts of the spontaneous polarizations in the (001)_C plane are switched to [001]_C direction, while others still stay in the (001)_C plane due to high induced internal stresses. Single domain state cannot be achieved even under a high electric field. After being poled along [001]_C, the volume fraction of domains with polarizations in the (001)_C plane is still about 25.2%. The extrinsic contributions to the dielectric constant are 15.7% and 27.2% under the *E* field of 1 kV/cm and under 2 kV/cm, respectively, estimated by the Rayleigh analysis. © 2015 AIP Publishing LLC. [<http://dx.doi.org/10.1063/1.4928756>]

(K, Na)NbO₃ (KNN) based piezoelectric materials have been extensively studied in the last decade as lead-free alternatives to PZT ceramics due to their high Curie temperature ($T_C > 300^\circ\text{C}$) and high piezoelectricity ($d_{33} > 300$ pC/N).¹⁻⁴ Great improvement in electrical performance has been made in recent years, focusing on the modification of compositions and optimization of preparation techniques.^{5,6} In general, the dielectric and piezoelectric properties can be divided into two parts: intrinsic and extrinsic contributions. The intrinsic response is related to the relative ionic shift that preserves the crystal structure orientation and crystal lattice symmetry, while the extrinsic response is ascribed to the domain wall motions.^{7,8} The extrinsic contribution plays a critical role in various functionalities, such as dielectric properties, piezoelectric activity, and energy loss behavior.^{9,10} In addition, understanding the mechanism of domain wall motions is very helpful to get some insight into the nonlinearity, frequency dispersion, and aging of physical properties.¹¹ For the investigation of domain structures, single crystals are preferred over ceramics because dynamic process of domain evolution with *E* field and temperature can be easily observed in single crystals. Up to date, studies on the domain evolution in KNN based materials are still limited due to the lack of available good quality single crystals, especially extrinsic contributions to dielectric and piezoelectric properties have not been quantified. In order to gain further insight into the high electromechanical properties of KNN-based materials, it is necessary to study domain evolution and to

determine the level of extrinsic contributions. In our previous work, large-sized high quality KNN-based single crystals with different compositions have been grown by the top-seeded solution growth (TSSG) method, which allowed us to carry out further research on domain configurations and extrinsic responses.¹²⁻¹⁶

Above room temperature, KNN materials are either in the orthorhombic phase or tetragonal phase. Compared with orthorhombic phase, the domain structure of tetragonal phase is simpler due to its higher symmetry. Therefore, it is easier to analysis the dynamic process of domain evolution and polarization rotation in tetragonal KNN. In this work, we focus on the tetragonal (K, Na, Li)(Nb, Sb, Ta)O₃ (KLNST) single crystal. The evolution of domain configuration with *E* field was studied by the polarizing light microscopy (PLM), and the extrinsic contribution to dielectric properties was delineated using the Rayleigh analysis.

All samples were oriented along pseudo-cubic (001)_C directions by X-ray diffraction method. The two (001)_C surfaces of the sample used for domain observations were polished into optical quality. Afterward, all samples were annealed at 600 °C for 1 h to eliminate internal stresses induced by cutting and polishing. Transparent conductive films of indium tin oxide (ITO) were deposited on the two (001)_C surfaces by magnetron sputtering for the *in situ* observation of domain structure evolution with *E* field. During the observation, the polarizer was always perpendicular to the analyzer. The light was propagating along [001]_C, the same direction as the applied *E* field. Domain structures were observed on the (001)_C surface. The experimental configuration is illustrated in Fig. 1(a). For samples used for electrical

^{a)}Authors to whom correspondence should be addressed. Electronic addresses: zhenglm@hit.edu.cn and binyang@hit.edu.cn.

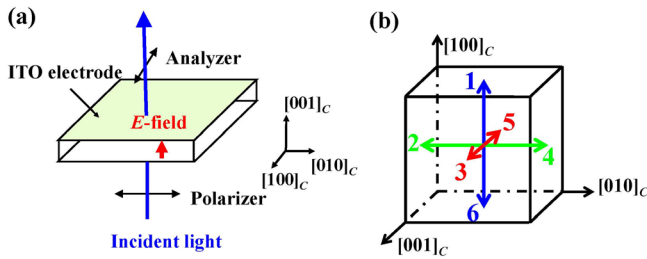


FIG. 1. (a) The observed domain configuration by PLM. (b) Schematic of six possible spontaneous polarizations in the tetragonal phase before being poled.

property measurements, gold electrodes were vacuum sputtered on the two $(001)_C$ surfaces. Poling was carried out under a field of 25 kV/cm for 15 min in silicone oil at room temperature. The dielectric constant was determined using an HP 4284D multi-frequency LCR meter. Polarization-electric loops were measured using a Precision Premier II tester (Radiant Tech., USA) at the frequency of 2 Hz.

The KNLNST single crystal is in the tetragonal phase at room temperature.¹⁴ The spontaneous polarizations (P_S) are along six $\langle 001 \rangle_C$ directions (denoted by 1, 2, ..., and 6), as shown in Fig. 1(b), and both 90° and 180° domains are permissible. In this work, P_S , which is along a particular direction N ($N = 1, 2, \text{ and } 6$) in Fig. 1(b), is written as $P_S \#N$. The angle between $[100]_C$ direction on the crystal and the polarizer is defined as θ .

The observation of domain configurations using PLM is based on the birefringence of the crystal.^{17–19} When a single domain crystal is placed between the mutually perpendicular polarizer and analyzer, the transmitted light intensity I is given by²⁰

$$I = I_0 \sin^2 2\alpha \sin^2 \frac{\varphi}{2}. \quad (1)$$

Here, I_0 is the incident light intensity into the sample, α is the angle between the polarizer and the projection of P_S at the plane perpendicular to the light propagation direction, and φ is the phase difference between the ordinary (o) and extraordinary (e) lights formed in the crystal, which can be expressed by

$$\varphi = \frac{360^\circ}{\lambda} (n_1 - n_2)t, \quad (2)$$

where λ is the wavelength of the light in vacuum, t is the thickness of the domain, and $(n_1 - n_2)$ is the planobirefringence. According to Eqs. (1) and (2), the intensity I depends on both t and α . For a certain domain with fixed thickness t , the maximum intensity should be achieved at $\alpha = 45^\circ$ and minimum ($I = 0$) at $\alpha = 0^\circ$. So, for domains with $P_S \#2, \#3, \#4, \text{ and } \#5$, the maximum intensity corresponds to $\theta = 45^\circ$, while complete extinction occurs at $\theta = 0^\circ$. For domains with $P_S \#1$ and $\#6$, the birefringence does not happen since the P_S is parallel to the light propagation direction, resulting in complete extinction at all angles. Based on the above analysis, it can be inferred that the 180° domain cannot be identified by PLM.

In most cases, domain layers overlap with each other in a sample. Domains with $P_S \#2, \#3, \#4, \text{ and } \#5$ all show

maximum intensity at $\theta = 45^\circ$ and extinction at $\theta = 0^\circ$. Overlapping of these domains will affect only the transmitted intensity, but not the extinction and maximum intensity position. Similarly, overlapping of domains with $P_S \#1$ and $\#6$ will also show complete extinction at all angles. When a domain with P_S in the $(001)_C$ plane overlaps a domain with P_S perpendicular to this plane, e.g., a $P_S \#1$ domain overlaps with a $P_S \#3$ domain, the light intensity and polarized direction will not change when propagate through the $P_S \#1$ domain. After passing through the $P_S \#3$ domain and analyzer, the intensity I can also be expressed by Eq. (1), and the phase difference is also formulated by Eq. (2). This domain structure shows maximum intensity at $\theta = 45^\circ$ and extinction at $\theta = 0^\circ$. It should be noted that the domain wall between the two domains is parallel to the $(101)_C$ plane (charged domain wall) or $(\bar{1}01)_C$ plane (neutral domain wall), which means that the thickness of $P_S \#3$ domain changes continuously from 0 to a maximum value t_0 , leading to the gradual change of light intensity.

Fig. 2 shows the evolution of domain structure an E field along $[001]_C$. All images were taken at $\theta = 45^\circ$. Before application of the E field, as shown in Fig. 2(a), most domain walls are along $[110]_C$ (denoted by S_1) and $[1\bar{1}0]_C$ (denoted by S_2). These are all 90° domain walls. These two kinds of domain walls are formed between P_S in the $(001)_C$ plane. Figs. 3(a) and 3(b) show the formation of S_1 and S_2 , respectively. With the application of the E field, more polarizations switched to $[001]_C$. As a result, the volume fraction of $P_S \#1$ domains increases. When the E field increases to 8 kV/cm, the nucleation of $P_S \#1$ domain can be observed, corresponding to the extinction region in Fig. 2(b). With further increase of the E field, the extinction region is enlarged. At the same time, the amount of S_1 and S_2 domain walls decreased, while the S_3 domain wall along $[010]_C$ appears, as shown in Figs. 2(c) and 2(d). Judging from the domain wall direction and the light intensity, the S_3 domain wall should be formed between $P_S \#1$ and $\#5$, or between $P_S \#1$ and $\#3$, as shown in Fig. 3(c). When the E field reaches 21 kV/cm, all S_1 and S_2 domain walls disappear, only S_3 domain walls remain (Fig. 2(f)). Further increase of the E field will not induce any marked changes in domain structures. As the E field decreases from 25 kV/cm, domain structures do not show essential changes until $E = 10$ kV/cm. With further decrease of the E field, more polarizations return to the $(001)_C$ plane, so that the extinction region decreases (Figs. 2(i) and 2(k)).

There are still S_3 domain walls in Fig. 2(g), indicating that single domain state is difficult to achieve. We also confirmed that the single domain state could not be obtained even by the high temperature poling process (above T_C then cooled under field). Generally speaking, domain switching is difficult in materials with high lattice anisotropy. The lattice parameters of the KNLNST single crystal calculated from X-ray diffraction pattern (not shown here) are $a = 3.9780 \text{ \AA}$ and $c = 4.0186 \text{ \AA}$. The c/a ratio is 1.010, comparable to that of tetragonal Pb-based relaxor single crystals.²¹ It is puzzling that the polarization switching in Pb-based crystals seems easier than that in KNLNST, in which single domain state can be obtained by the room temperature or high temperature poling processes.^{22–24} When polarizations in $(001)_C$ plane

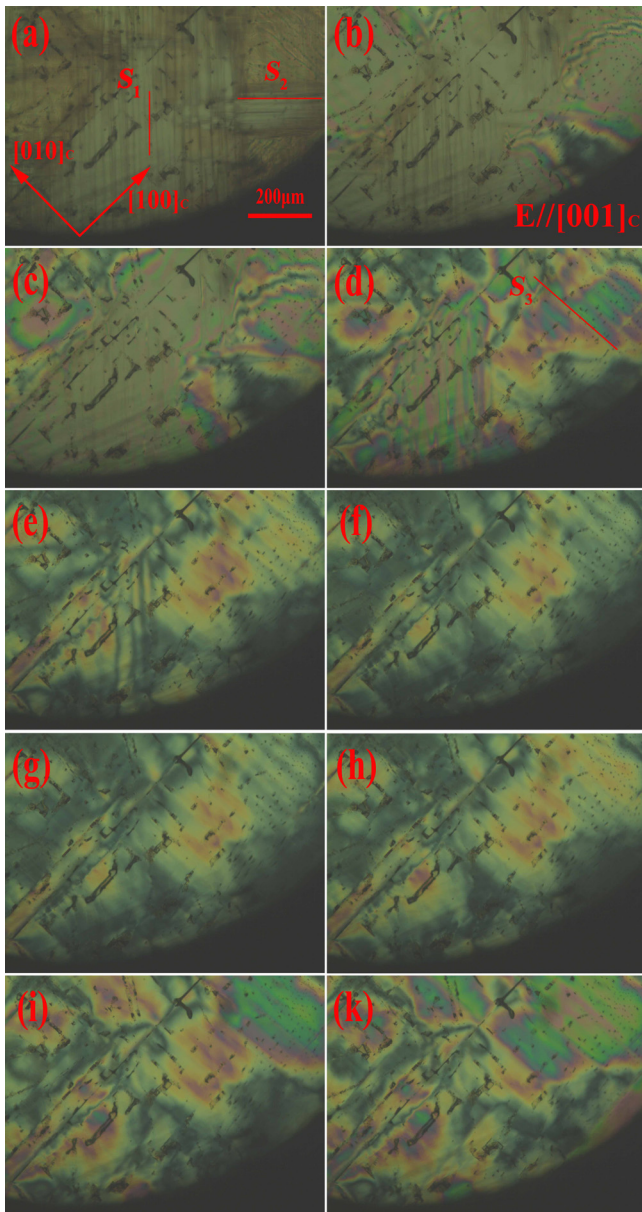


FIG. 2. E field dependent domain structures observed at room temperature. (a) 0 kV/cm, (b) 8 kV/cm, (c) 17 kV/cm, (d) 19 kV/cm, (e) 20 kV/cm, (f) 21 kV/cm, and (g) 25 kV/cm during the field increasing process, and (h) 10 kV/cm, (i) 5 kV/cm, and (k) 0 kV/cm during the field decreasing process.

rotate toward $[001]_C$, the strain S_4 will be induced, resulting in the formation of internal stress T_4 . The relationship is

$$T_4 = c_{44}S_4, \quad (3)$$

where c_{44} is the shear elastic stiffness constant. Since KNLNST and PbTiO_3 (PT)-based crystal show comparable

lattice anisotropy, similar S_4 will be formed if the in plane polarizations rotate by the same angle. c_{44} of KNLNST cannot be measured for the lack of single domain sample. According to our previous work, c_{44}^E and c_{55}^E of single domain orthorhombic KNN-based crystal are 7.80×10^{10} and 1.90×10^{10} N/m², respectively, more than 5 times larger than those of the Pb-based crystals with the same domain structure ($c_{44}^E = 1.28 \times 10^{10}$ and $c_{55}^E = 0.32 \times 10^{10}$ N/m²).^{25,26} So, we may conclude that in the tetragonal phase, c_{44} of KNLNST should be much larger than that of the Pb-based crystals. Larger stress T_4 formed in KNLNST crystal prevents further polarization rotation, so that the single domain state is hard to achieve.

The extent of poling greatly affects the electromechanical properties. Thus, it is important to estimate the percentage of the remaining polarizations in the $(001)_C$ plane in a poled sample. In theory, it can be estimated from Fig. 2 by calculating the area of extinction regions in the images.¹⁶ However, the transmitted light intensity may be affected by many factors, such as overlapping of domains, scattering of domain walls, and interference from the transmitted light. So, there would be a large error if it is calculated by this method. Therefore, this method was not used here. Instead, the following method, which is based on the dielectric properties, was adopted.

Before poling, the probabilities of the 6 polarizations are equal. So, the volume fraction of domains with P_S in the $(001)_C$ plane is $2/3$, and the volume fraction of domains with P_S #1 and #6 is $1/3$. We assume that the two independent dielectric constants of ideal single domain state, e.g., longitudinal and transverse dielectric constants, are ϵ_{33}^{sd} and ϵ_{11}^{sd} , respectively. The dielectric constant for an unpoled sample along $[001]_C$ is defined as ϵ_r . It can be inferred that ϵ_r should be the combined effect of all domains. For domains with P_S #1 and #6, their contributions to ϵ_r are ϵ_{33}^{sd} , while for domains with P_S #2, #3, #4, and #5, the effective dielectric constant should be ϵ_{11}^{sd} . The arrangement of different domains will also affect ϵ_r . The overlapping of domains along the thickness direction $[001]_C$ is unavoidable. Here, we divide the domains into two types, Type A are domains with P_S in the $(001)_C$ plane, while Type B are domains with P_S #1 and #6. When A domains overlap with each other, the total dielectric properties along $[001]_C$ do not change due to the same dielectric constants of all the domains. It is the same situation when B domains overlap with each other. However, when an A domain overlaps with a B domain, serial capacitors are formed and the total dielectric constant should be changed. It should be noted that the volume fraction of the two types of domains that overlapped with each other should be very small due to the fact that the sample is

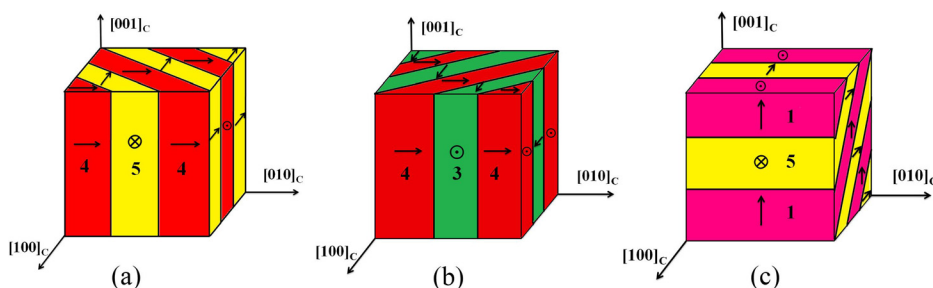


FIG. 3. Schematic of (a) domain wall S_1 (neutral domain wall between P_S #4 and #5), (b) domain wall S_2 (neutral domain wall between P_S #4 and #3), and (c) domain wall S_3 (charged domain wall between P_S #1 and #5).

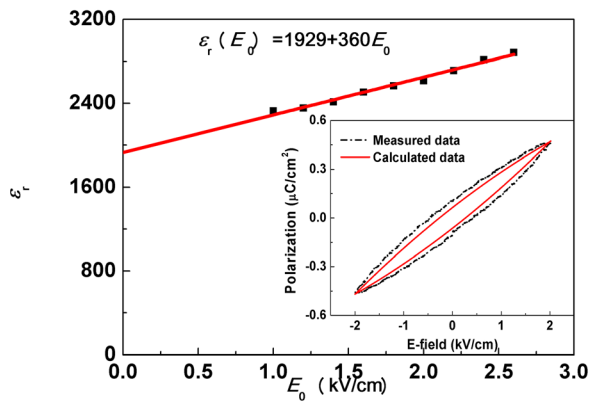


FIG. 4. Electric field dependence of dielectric permittivity $\epsilon_r'(E_0)$ for the unpoled KNLNST single crystal. The inset shows the comparison between the measured and calculated P - E hysteresis loop.

very thin ($3.0 \text{ mm} // [100]_C \times 3.0 \text{ mm} // [010]_C \times 0.3 \text{ mm} // [001]_C$). So, the contribution from serial capacitors is negligible. In addition, the contribution of the domain walls to ϵ_r is also neglected. In other words, we just considered the situation of parallel capacitors. The following relationship may be obtained:

$$\epsilon_r = \frac{2}{3}\epsilon_{11}^{sd} + \frac{1}{3}\epsilon_{33}^{sd}. \quad (4)$$

After being poled, parts of the P_S #2, #3, #4, and #5 are switched to become P_S #1. We assume that the total volume fraction of A domains is x , so the volume fraction of B domains is $1-x$. The longitudinal dielectric constant will become

$$\epsilon_{33} = x \cdot \epsilon_{11}^{sd} + (1-x) \cdot \epsilon_{33}^{sd}. \quad (5)$$

In our case, ϵ_r and ϵ_{33} are determined to be 2016 and 912, respectively. ϵ_{11}^{sd} and ϵ_{33}^{sd} cannot be directly measured due to the lack of single domain sample. In another tetragonal KNN based single crystal, $(\text{K}, \text{Na}, \text{Li})(\text{Nb}, \text{Ta})\text{O}_3$, the single domain state can be achieved, and the measured ϵ_{33}^{sd} is around 240. Considering that the two crystals show similar phase transition temperature ($T_{O-T} = 23^\circ\text{C}$, $T_C = 197^\circ\text{C}$ for $(\text{K}, \text{Na}, \text{Li})(\text{Nb}, \text{Ta})\text{O}_3$ and $T_{O-T} = -10^\circ\text{C}$, $T_C = -210^\circ\text{C}$ for KNLNST),¹⁴ and both crystals are stable in the tetragonal phase at room temperature, it is reasonable to assume that ϵ_{33}^{sd} of KNLNST is around 240, then ϵ_{11}^{sd} is calculated to be around 2904 through Eq. (4), and x should be 25.2% according to Eq. (5). Because ϵ_{33}^{sd} is much smaller than ϵ_{11}^{sd} , slight change of its value will not affect the conclusion.

In order to understand the contribution of domain wall motions to the dielectric constant, the Rayleigh analysis has been performed on the KNLNST single crystal^{27,28}

$$\epsilon_r'(E_0) = \epsilon_{r'init}' + \alpha E_0, \quad (6)$$

$$P = \epsilon_0[(\epsilon_{r'init}' + \alpha E_0)E \pm \alpha(E_0^2 - E^2)/2]. \quad (7)$$

Here, E_0 is the amplitude of the electric field, $\epsilon_r'(E_0)$ is the dielectric constant under E_0 , $\epsilon_{r'init}'$ is the intrinsic portion of the dielectric constant, P is the polarization under electric field E , ϵ_0 is the vacuum dielectric permittivity ($8.854 \times 10^{-12} \text{ F/m}$), and α is the Rayleigh parameter. The term

αE_0 represents the extrinsic contribution to the total dielectric constant, $\epsilon_r'(E_0)$ can be calculated from the peak-to-peak polarization in P - E hysteresis loop, as shown in the inset of Fig. 4, $\epsilon_{r'init}'$, and α can be obtained by fitting the $\epsilon_r'(E_0)$ curve using Eq. (6), which were found to be 1929 and 360 cm/kV, respectively, as shown in Fig. 4. It can be concluded that the extrinsic contribution to the total dielectric response is 15.7% at $E_0 = 1 \text{ kV/cm}$ and increases to 27.2% at $E_0 = 2 \text{ kV/cm}$. The extrinsic contribution is much larger than that of the $0.95(\text{K}_{0.5}\text{Na}_{0.5})\text{NbO}_3-0.05\text{LiTaO}_3$ ceramics, which is lower than 10% in the tetragonal phase.²⁹ Domain wall motions should be more active in single crystals than in ceramics due to the nonexistence of grain boundaries, resulting in higher extrinsic contributions in single crystals.

In summary, we have studied the E field induced domain evolution in tetragonal KNLNST single crystal. It was found that single domain state cannot be achieved due to the large shear elastic stiffness constant c_{44} . By comparing the dielectric constants of poled and unpoled samples, the volume fraction of domains with polarizations remaining in the $(001)_C$ plane was estimated to be 25.2%. Based on the Rayleigh analysis, the extrinsic contribution to the dielectric constant in the unpoled sample can be extracted to be 15.7% under the E field of 1 kV/cm and increase to 27.2% under the E field of 2 kV/cm.

This work was supported by the National Key Basic Research Program of China (Grant No. 2013CB632900), the NIH under Grant No. P41-EB21820, the PIRS of HIT (Grant No. B201509), the National Science Foundation of China (Grant Nos. 51102062 and 11372002), and the Key Technologies R&D Program of China (Grant No. 2013BAI03B06).

- ¹S. Yasuyoshi, T. Hisaaki, H. Toshihiko, N. Tatsuhiko, T. Kazumasa, H. Takahiko, N. Toshiatsu, and N. Masaya, *Nature* **432**, 84 (2004).
- ²J. Rödel, W. Jo, K. T. P. Seifert, E. M. Anton, T. Granzow, and D. Damjanovic, *J. Am. Ceram. Soc.* **92**, 1153 (2009).
- ³J. Li, K. Wang, F.-Y. Zhu, L.-Q. Cheng, and F.-Z. u. Yao, *J. Am. Ceram. Soc.* **96**, 3677 (2013).
- ⁴T. Shrout and S. Zhang, *J. Electroceram.* **19**, 113 (2007).
- ⁵X. Wang, J. Wu, D. Xiao, J. Zhu, X. Cheng, T. Zheng, B. Zhang, X. Lou, and X. Wang, *J. Am. Ceram. Soc.* **136**, 2905 (2014).
- ⁶K. Wang, F.-Z. Yao, W. Jo, D. Gobeljic, V. Shvartsman, D. Lupascu, J.-F. Li, and J. Rödel, *Adv. Funct. Mater.* **23**, 4079 (2013).
- ⁷G. Arlt and N. Pertsev, *J. Appl. Phys.* **70**, 2283 (1991).
- ⁸L. Zheng, X. Yi, S. Zhang, W. Jiang, B. Yang, R. Zhang, and W. Cao, *Appl. Phys. Lett.* **103**, 122905 (2013).
- ⁹T. Sluka, A. K. Tagansev, D. Damjanovic, M. Gureev, and N. Setter, *Nat. Commun.* **3**, 748 (2012).
- ¹⁰G. Liu, S. Zhang, W. Jiang, and W. Cao, *Mater. Sci. Eng., R* **89**, 1 (2015).
- ¹¹D. Damjanovic, *J. Am. Ceram. Soc.* **88**, 2663 (2005).
- ¹²L. Zheng, X. Huo, R. Wang, J. Wang, W. Jiang, and W. Cao, *CrystEngComm* **15**, 7718 (2013).
- ¹³X. Huo, L. Zheng, R. Zhang, R. Wang, J. Wang, S. Sang, Y. Wang, B. Yang, and W. Cao, *CrystEngComm* **16**, 9828 (2014).
- ¹⁴J. Wang, L. Zheng, B. Yang, R. Wang, X. Huo, S. Sang, J. Wu, Y. Chang, H. Ning, T. Lv, and W. Cao, *J. Cryst. Growth* **409**, 39 (2015).
- ¹⁵X. Huo, R. Zhang, L. Zheng, S. Zhang, R. Wang, J. Wang, S. Sang, B. Yang, and W. Cao, *J. Am. Ceram. Soc.* **98**, 1829 (2015).
- ¹⁶L. Zheng, J. Wang, X. Huo, R. Wang, S. Sang, S. Li, P. Zheng, and W. Cao, *J. Appl. Phys.* **116**, 044105 (2014).
- ¹⁷D. Zekria, V. Shuvaeva, and A. Glazer, *J. Phys.: Condens. Matter* **17**, 1593 (2005).
- ¹⁸D. Zekria and A. Glazer, *J. Appl. Crystallogr.* **37**, 143 (2004).

- ¹⁹L. Zheng, X. Lu, H. Shang, Z. Xi, R. Wang, J. Wang, P. Zheng, and W. Cao, *Phys. Rev. B* **91**, 184105 (2015).
- ²⁰A. K. Tagantsev, L. E. Cross, and J. Fousek, *Domains in Ferroic Crystals and Thin Films* (Springer, New York, 2010), pp. 161–172.
- ²¹A. Singh and D. Pandey, *Phys. Rev. B* **67**, 064102 (2003).
- ²²H. Cao, V. Schmidt, R. Zhang, W. Cao, and H. Luo, *J. Appl. Phys.* **96**, 549 (2004).
- ²³F. Li, S. Zhang, Z. Xu, X. Wei, J. Luo, and T. Shrout, *J. Appl. Phys.* **107**, 054107 (2010).
- ²⁴S. Zhang, C. Randall, and T. Shrout, *Solid State Commun.* **131**, 41 (2004).
- ²⁵L. Zheng, S. Li, S. Sang, J. Wang, X. Huo, R. Wang, Z. Yuan, and W. Cao, *Appl. Phys. Lett.* **105**, 212902 (2014).
- ²⁶S. Zhang, G. Liu, W. Jiang, J. Luo, W. Cao, and T. Shrout, *J. Appl. Phys.* **110**, 064108 (2011).
- ²⁷R. Eitel, T. Shrout, and C. Randall, *J. Appl. Phys.* **99**, 124110 (2006).
- ²⁸D. Damjanovic, *Phys. Rev. B* **55**, R649 (1997).
- ²⁹B. Peng, Z. Yue, and L. Li, *J. Appl. Phys.* **109**, 054107 (2011).